Asian Journal of Chemistry; Vol. 38, No. 1 (2026), 173-179
ASIAN JOURNAL OF CHEMISTRY
https://doi.org/10.14233/ajchem.2026.34994

Biosynthesis of Rice Starch-Manganese Dioxide (IV) Nanocomposite: Its Characterization and Biological Potential

GEETANJALI[1], B. CHANDRA[1,*], J. PRASAD[2], A. TAMTA[3] and N.D. KANDPAL[1]

[1]Department of Chemistry, Kumaun University Nainital, S.S.J. Campus Almora-263601, India
[2]Department of Chemistry, Government Post Graduate College (Affiliated to Kumaun University), Sitarganj-262405, India
[3]Department of Chemistry, S.S.H.D. Government Degree College Agrora (Affiliated to Sri Dev Suman Uttarakhand University), Dharmandal, Tehri Garhwal-249127, India

*Corresponding author: E-mail: bc_physical@rediffmail.com

Received: 1 October 2025 *Accepted*: 18 November 2025 *Published online*: 31 December 2025 AJC-22235

Manganese dioxide (MnO_2) nanoparticles were biosynthesized in this study, utilizing rice starch (a natural polymer) to form nanocomposites with useful biological and analytical properties. The synthesized nanocomposites were characterized by XRD, FTIR, UV-Vis, HRTEM, FESEM-EDX and Zeta potential analysis. FTIR confirmed the formation of rice starch-manganese dioxide (rice starch-MnO_2) nanocomposites and the presence of functional groups in the synthesis. XRD analysis determined the average crystalline size to be 38.27 nm, while FESEM and HRTEM revealed a spherical structure with irregular morphology. EDX confirmed a presence of manganese content 43.12%, oxygen 29.02% and carbon 27.86%. The anticancer activity against the HepG2 cell line (a human liver cancer cell line) was determined by MTT Assay, with an IC_{50} value of 76.31 ± 0.092 µg/mL. Antioxidant activity shows appreciable potency in the DPPH scavenging assay. The nanocomposites were thought to be stable under thermal conditions and to have prominent antioxidant and anticancer properties.

Keywords: Rice starch-MnO_2 nanocomposite, Nanoparticles, Anticancer activity, Antioxidant activity.

INTRODUCTION

In recent years, MnO_2 nanoparticles have garnered considerable attention due to their potential in various biomedical applications, including antibacterial [1], biomedical [2], drug delivery [3] and biosensing [4]. Previous studies on nanoparticles of metals and metal oxides have extensively investigated various biological applications. MnO_2 nanoparticles have been the focus of research due to their low potential cytotoxicity compared to other metal oxide nanoparticles [5]. Due to the abundant natural availability and renewability of these natural polymers, like proteins, polysaccharides such as cellulose, starch and glycogen, *etc*. current research is focused on developing biopolymer-based nanocomposites with starch.

Nowadays, many methods have been used, including electrochemical, catalytic and electro-catalytic biosensors that utilize the non-toxic, low-cost and abundant manganese oxides [6]. It is well known that metals can produce a wide range of oxides due to their exceptional physico-chemical properties, especially their high thermal stability, catalytic activity, effective biological qualities and ability to form nanocomposites [7,8]. According to earlier studies, polymers are more suited for creating biopolymer-based nanocomposites due to their inherent availability and renewability [9]. Significant biological capabilities have been shown by nanoparticles bonded to the surface of other metals or metal oxides and mixed with polymers to create nanocomposites, as opposed to nanoparticles alone [10].

Plants use starch, a naturally occurring, edible and biodegradable carbohydrate, as their main energy source. Every year, photosynthesis produces around 2,850 million tons of starch worldwide. Plants contain it and key crops including wheat, rice, potatoes, corn and tapioca are rich sources of it. Due to its renewability, biocompatibility and versatile physicochemical properties, starch has been widely used in various industrial sectors, including food and beverages, pharmaceuticals and cosmetics, plastics, textiles, construction and paper manufacturing [11]. Rice is mostly composed of starch, which accounts for about 80% of its contents. It consists of monosaccharide units that form amylose and amylopectin. It

is generally known that amylose and amylopectin play important roles in the gelatinization and pasting of rice starch. The impact of starch content on the regulation of manganese dioxide's size, shape and structure, however, has not received much attention. Consequently, the goal of the current work is to easily synthesize MnO_2 nanoparticles by employing rice starch as a green capping agent that acts as a terminator for particle growth. Furthermore, the nanostructural aspect of MnO_2 nanoparticles was modified by varying the quantity of rice starch [12]. PEG was used to coat the nanoparticles, enhancing their physico-chemical characteristics and enhancing their biological activity for biomedical applications. PEG coating stabilizes nanoparticles, reduces toxicity and improves their biocompatibility [13].

This study is concerned with the biosynthesis and biological properties of rice starch-MnO_2 nanocomposites, which are based on natural polymers. The phase, the structure and the morphology of the synthesized rice starch-manganese oxide nanocomposites were characterized by spectroscopic techniques, XRD, FTIR, UV-Vis, HRTEM, FESEM-EDX and zeta potential. The biological properties like anticancer and antioxidant activity were also investigated.

EXPERIMENTAL

Analytical grade solvents were used in this work. Manganese chloride (Fine Chemicals), potassium permanganate (Laboratory reagents), polyethylene glycol (PEG 4000) from Merck Ltd. India and rice from the local market and Soapnut (reetha) were used to prepare nanocomposites. Distilled water was used throughout the experiment for solution preparation and for washing purposes.

Synthesis of MnO_2 nanoparticles: By employing $MgCl_2$, 1.88 g in 45 mL of double-distilled water with a required amount of 5 mL methanolic extract of *Sapindus mukorossi* (reetha/soapnut). $KMnO_4$ (2.38 g) dissolved in 50 mL of distilled water, while being continuously stirred by a magnetic stirrer for 1 h at room temperature. After filtering and washing with ethanol and double-distilled water, the resultant black precipitate was left to air for 24 h. Then, the powdery black precipitate of MnO_2 nanoparticle was dried for 15 h at 80 ºC.

Starch extraction: In order to extract starch, the local rice was cleaned and ground into a powder after being bought from a local market in Bhatronjkhan, Almora district of India. A modified alkaline extraction procedure [14] was used to extract the starch.

Protein and starch isolation: Aqueous NaOH (800 mL) and a concentration of 0.05 M NaOH was combined with 160 g of dry rice flour. After 3 h of stirring at 25 ºC, the material was left to settle for 24 h. The protein-containing yellow liquid supernatant was decanted. The residue was blended for 15 min, followed by the addition of 500 mL of 0.05 M NaOH solution and the mixture was kept at 25 ºC for 3 h before being stored overnight at room temperature. This process was repeated until the yellow layer was completely removed. The alkaline slurry was then neutralized with 1.0 M HCl and centrifuged. The resulting starch slurry was washed with a 1:1 (v/v) ethanol–water mixture and centrifuged again. The purified starch was dried in an oven at 35-40 ºC for 48 h and stored in an airtight container.

Synthesis of rice starch-MnO_2 nanocomposites: Rice starch (1.5 g) in 50 mL of double-distilled water was stirred at 35 ºC for 30 min to obtain a saturated solution. To prepare MnO_2 nanoparticles (0.25 g) dissolved in 35mL of distilled water, to make up the total volume of the solution to 50 mL, a mixture of PEG 4000 (0.1 g) in 5mL of distilled water and 10 mL of methanolic extract, was added. Separate addition of each solution result in distinct solvent behaviour to form a ternary solvent system. Adding this mixture dropwise to the saturated starch solution, which formed a brown precipitate. The obtained precipitate was left untouched overnight and then centrifuged at 4000 rpm for 15 min. The precipitate was decanted and washed with ethanol and water for 2 times, then dried at 80 ºC for 2 h.

Characterization: The characterization of rice starch-MnO_2 nanocomposites was recorded by XRD (PW3050/60 X-ray diffractometer) while FT-IR analysis (Perkin-Elmer 2) was performed to identify the functional groups present in the synthesized material. To detect the surface charge of particles, zeta potential was measured using LENOVO Litesizer 500, an advanced cumulant model. HRTEM was conducted with the JEOL model name: JEM 2100 plus. FESEM images and the corresponding EDX spectra were obtained using a JEOL JSM-6100 equipped with an image analyzer. The optical absorption properties of the rice starch-MnO_2 nanocomposites were analyzed using a Perkin-Elmer UV-Vis-NIR spectrophotometer (λ = 750 nm).

Anticancer activity: The anticancer activity was determined using the MTT assay against the HepG2 cell line. The cells (10000 cells/well) were cultured in 96-well plate for 24 h in DMEM medium (Dulbecco's Modified Eagle Medium-AT149-1L) supplemented with 10% FBS (Fetal Bovine Serum, HIMEDIA-RM 10432) and 1% antibiotic solution (penicillin-streptomycin, Sigma-Aldrich P0781) at 37ºC with 5% CO_2. At the end of experiment, culture supernatant was removed and cell layer matrix was dissolved in 100 µL dimethyl sulfoxide (DMSO) and read in an Elisa plate reader (iMark, Biorad, USA) at 540 nm and 660 nm.

$$\text{Viable cells (\%)} = \frac{A_{test}}{A_{control}} \times 100$$

where A_{test} = absorbance of test sample, $A_{control}$ = absorbance of control.

Antioxidant activity: The antioxidant activity content was determined according to the method of DPPH scavenging assay. A 10 µL of different stock of the test compound was added to 0.2 mL of 0.1 mM DPPH solution in methanol in a 96-well plate. Ascorbic acid was used as a standard. The reaction was set in quadruplicate form and duplicates of blank were prepared containing 0.2 mL DPPH and 10 µL standard/sample of different concentrations. The plate was incubated for 30 min in dark. At the end of incubation, the decolourization was read at 517 nm using a microplate reader (iMark, BioRad). Reaction mixture containing 20 µL of deionized water was served as the control. The scavenging activity was estimated as '%inhibition' with respect to the control. Further, the inhibited DPPH percentage was calculated by the following equation:

$$\text{DPPH\% RSA} = \frac{\text{Abs}_{\text{control}} - \text{Abs}_{\text{sample}}}{\text{A}_{\text{control}}} \times 100$$

where RSA = radical scavenging activity; $Abs_{control}$ = absorbance of control; and Abs_{sample} = absorbance of sample.

RESULTS AND DISCUSSION

X-ray studies: The XRD spectrum of the prepared rice starch-MnO_2 nanocomposites is shown in Fig. 1. The smaller peaks observed at 2θ values, 27.36º and 35.99º, in the XRD spectrum of rice starch-MnO_2 nanocomposites. The peak at 27.36º may be characteristic of rice starch. The average crystallite size (D) of nanocomposites was estimated to be 38.27 nm. The obtained pattern shows two noticeable peaks at 27.36º and 35.99º, assigned to *hkl* values (112) and (004), respectively [15]. The broadening of peaks indicates the sample is weakly crystalline or more amorphous. It confirms that the formation of MnO_2 nanoparticles was present in rice starch-MnO_2 nanocomposites.

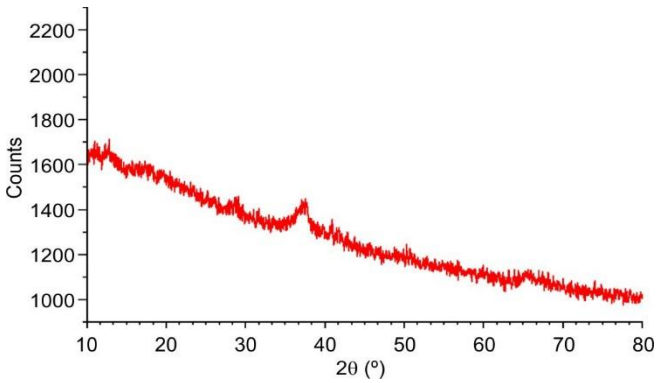

Fig. 1. XRD spectrum of rice starch-MnO_2 nanocomposite

FTIR spectral studies: The FT-IR spectrum of the rice starch-MnO_2 nanocomposite exhibits a broad absorption band at 3332 cm^{-1}, corresponding to the O–H stretching vibrations typical of polysaccharides such as starch. This band arises from hydroxyl groups present in the glucopyranose units of rice starch [16]. A characteristic absorption near 512 cm^{-1} (Fig. 2) falls within the metal–oxide region, confirming the successful incorporation of MnO_2 into the starch matrix. Weak absorption bands observed in the 2992-2167 cm^{-1} region is attributed to the asymmetric stretching vibrations of C–CH_2–C groups in starch. Moreover, the vibrations related to the deformation of hydroxyl groups from bound water molecules associated with the starch structure are also evident in this region [17]. In the fingerprint region, four distinct peaks between 1148 and 929 cm^{-1} correspond to skeletal vibrations of the pyranose ring. According to literature, IR bands within 1078-929 cm^{-1} are indicative of both the amorphous and crystalline domains of starch [18-20]. Overall, the spectral features clearly demonstrate the formation of a rice starch-MnO_2 nanocomposite. The band at 567 cm^{-1} can be assigned to Mn–O stretching vibrations, further confirming the presence of MnO_2 nanoparticles. Furthermore, minor bands surrounding the metal–oxide region arise from starch molecules coating the surface of the MnO_2 nanoparticles.

UV-Vis spectral studies: A UV-absorption spectrum ranging from 200 to 600 nm was obtained for the synthesized rice starch-MnO_2 nanocomposite. The UV–Vis spectrum of the rice starch–MnO_2 nanocomposite shows a strong absorption peak at 462 nm, which lies near the characteristic threshold region around 216 nm, as illustrated in Fig. 3. The direct band gap energy of the nanocomposite was calculated using the Tauc plot (inset Fig. 3), where the extrapolation of the linear portion of the curve onto the *x*-axis yielded a value of 1.38 eV. This result aligns well with earlier reports indicating that MnO_2-based nanocomposites with a band gap near 1.3 eV exhibit enhanced luminescence within the visible region [21].

FESEM-EDX studies: It is noteworthy that the surface functionalization of nanocomposites generally does not significantly influence their morphology or particle size [22]. As shown in Fig. 4 (EDX) and Fig. 5 (FESEM images, a-b), the

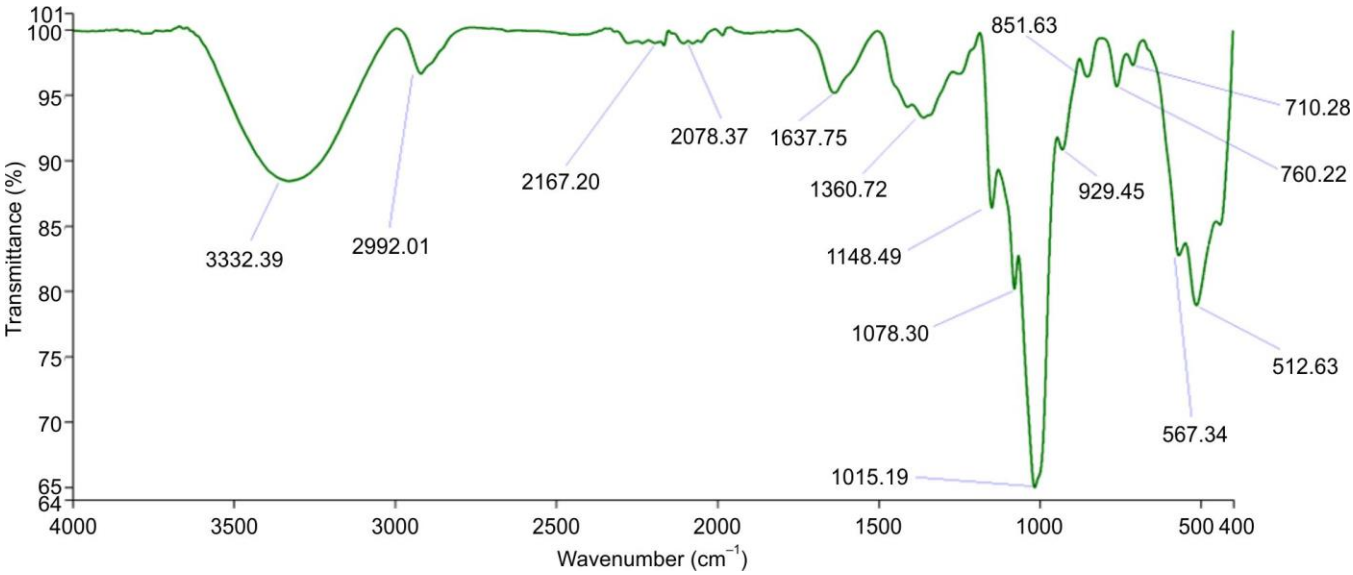

Fig. 2. FTIR spectrum of rice starch-MnO_2 nanocomposite

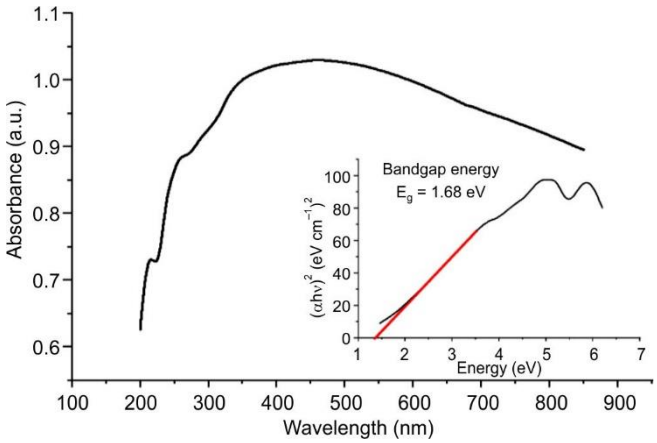

Fig. 3. UV-Vis spectrum and Tauc plot for band gap energy determination of rice starch-MnO_2 nanocomposite

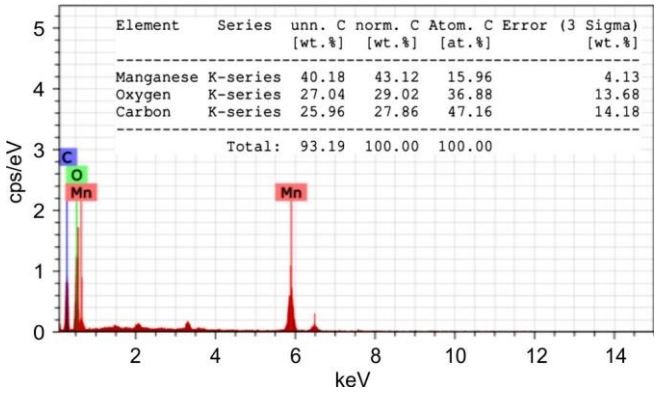

Fig. 4. EDX spectrum of rice starch-MnO_2 nanocomposite with the element details

rice starch-MnO_2 nanocomposites exhibit uniformly grown particles with predominantly spherical to oval morphologies. The nanoparticles appear moderately agglomerated yet remain well distributed across the composite surface, which is the characteristic of starch-stabilized metal oxide systems [23].

Energy-dispersive X-ray (EDX) analysis confirmed the elemental composition of the nanocomposite, revealing the mass percentages of Mn: 43.12%, O: 29.02%, and C: 27.86%. The presence of these elements, along with their relative proportions, validates the successful synthesis of the rice starch-MnO_2 nanocomposite and confirms the incorporation of MnO_2 within the starch matrix.

HRTEM studies: The HRTEM images of rice starch-MnO_2 nanocomposites (Fig. 6) showed the irregular spherical and some crystal structure. The scale bars of 50 nm, 100 nm, and 200 nm in the TEM images provide a reliable reference for estimating particle size, confirming that the synthesized materials fall within the nanoscale range. The TEM micrograph of the starch-MnO_2 nanocomposite displays a network-like architecture, which arises from the intrinsic chemical structure of starch and its tendency to promote particle aggregation through intermolecular interactions [24]. The overall particle distribution and morphology clearly demonstrate that the green synthesis approach successfully produced rice starch-MnO_2 nanocomposite with controlled size and shape. This uniformity highlights the effectiveness of starch as a natural stabilizing and structuring agent during nanoparticle formation.

Zeta potential: Fig. 7 shows the particle size distribution of the starch-MnO_2 nanocomposite, which allow to predict the relationship between ionic strength and zeta potential. The nanocomposite exhibits an average zeta potential of –16.5 mV, with a conductivity of 0.0264 mS/cm and a standard deviation of 3.97 mV. Although some degree of particle aggregation was observed, these values indicate that the rice starch-MnO_2 nanocomposite possesses moderate colloidal stability.

The addition of salts during the process promotes charge screening, which enhances particle aggregation and leads to the precipitation at lower concentrations, which is consistent with the behaviour of starch-stabilized metal oxide systems [25]. The nanocomposite displayed both positive and negative zeta potential values depending on the ionic environment, reflecting the surface heterogeneity contributed by starch functional groups. Overall, the measured zeta potential provides a useful indicator of the long-term stability and durability of the rice starch-MnO_2 nanocomposites.

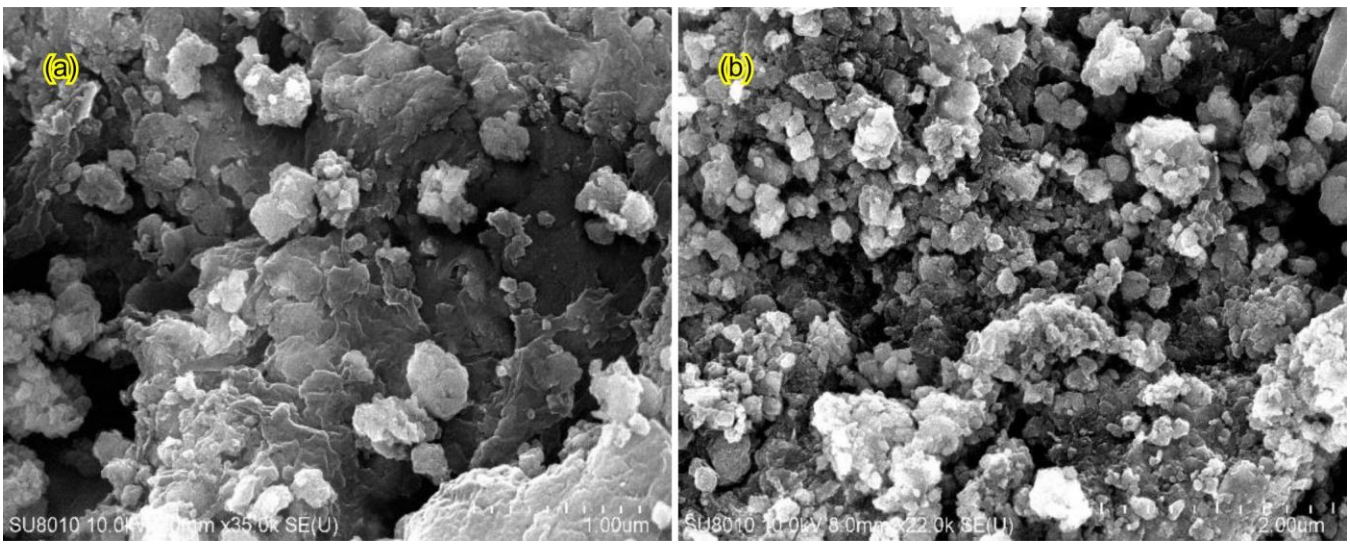

Fig. 5. FESEM micrographs of rice starch-MnO_2 nanocomposite at different magnifications

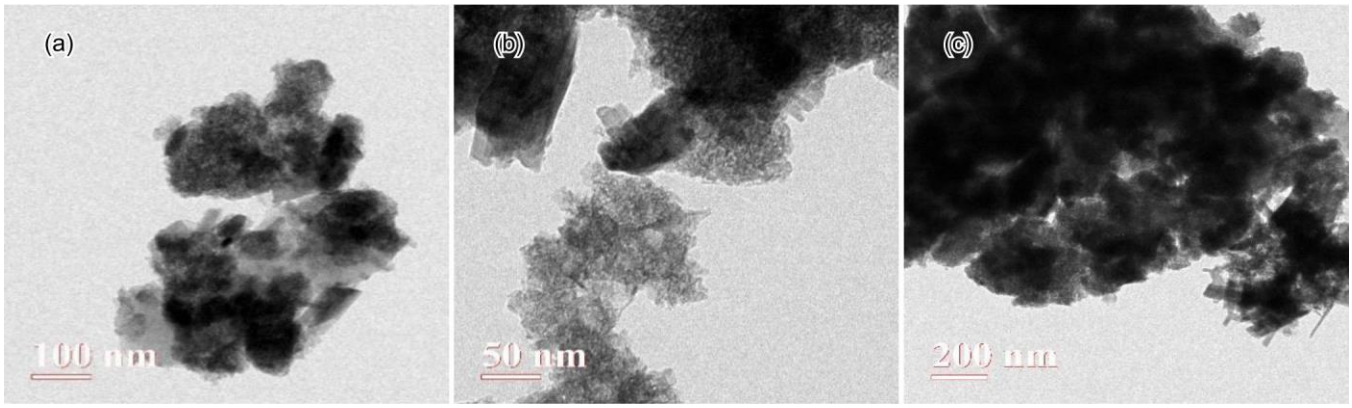

Fig. 6. HRTEM images of rice starch-MnO_2 nanocomposites in different nano-scale range (a) 100 nm, (b) 50 nm, (c) 200 nm

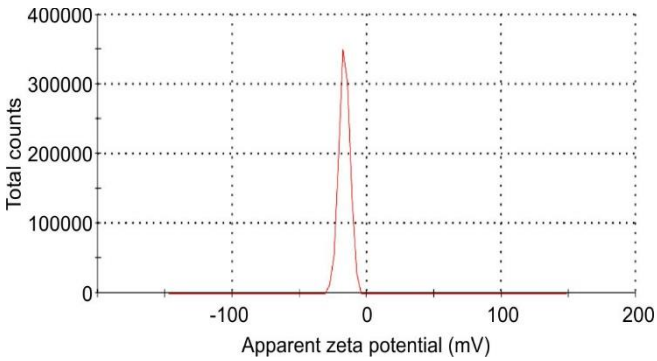

Fig. 7. Zeta potential graph of rice starch-MnO_2 nanocomposite

Anticancer activity: The cytotoxicity of the rice starch-MnO_2 nanocomposite against HepG2 liver cancer cells was evaluated using the MTT assay. Morphological observations revealed clear differences between untreated cells and those exposed to the nanocomposite, with treated cells showing progressive structural deterioration. HepG2 cells exposed to increasing concentrations of the nanocomposite (1-1000 µg/mL) exhibited a significant, dose-dependent increase in cell death. The IC_{50} value was calculated to be 76.31 ± 0.092 µg/mL, expressed as mean ± SEM, indicating substantial cytotoxic potency.

The dose-dependent decline in cell viability, as illustrated in Fig. 8, confirms the strong anticancer activity of the rice starch-MnO_2 nanocomposite. This effect may be attributed to the bioactive surface characteristics imparted by both the starch matrix and the biogenically synthesized MnO_2 nanoparticles, which can act as capping and stabilizing agents. Crystal violet staining, MTT assays, and microscopic examination of cell morphology collectively demonstrated the cytotoxic impact of the nanocomposite on HepG2 cells, with all methods consistently showing reduced viability at higher concentrations [26]. The enhanced cytotoxic response is likely related to the unique interactions between nanoparticles and cellular components, which can disrupt metabolic and structural processes [27,28]. Although these findings are promising, the present study was limited to the HepG2 cell line. To better establish the therapeutic potential and broad-spectrum anticancer activity of rice starch-MnO_2 nanocomposites, further studies should evaluate their effects on additional liver-derived and non–liver derived cancer cell lines [29].

Antioxidant activity: DPPH assay was used to evaluate the capacity of rice starch-MnO_2 nanocomposite to neutralize free radicals at different doses. DPPH is typically neutralized by absorbing hydrogen from a hydrogen donor molecule or electron transfer nanoparticles. The violet colour of the reaction mixture decreases when DPPH is reduced, indicating the presence of NPs that scavenge free radicals [30]. The IC_{50} was found to be 12.82 ± 0.02 for the standard solution. The standard compound, being a purified compound and highly active substance, was assessed using a lower concentration range (0 to 50 µg/mL). However, the efficacy of rice starch-MnO_2 nanocomposite is still unbound, hence a wider concentration range (0 to 1000 µg/mL) was used as shown in Fig. 9b. Based on the results obtained from the experimental work, the antioxidant activity (DPPH assay) was accurately estimated.

The percentage inhibition of antioxidant activity for both the standard and the rice starch-MnO_2 nanocomposite was plotted against their respective concentrations. When compared with the reference antioxidant ascorbic acid (IC_{50} = 12.82 ± 0.02 µg/mL), the nanocomposite exhibited only modest inhibitory activity toward the DPPH radical. This limited activity is reflected in its comparatively higher IC_{50} value.

The antioxidant effect observed in the rice starch-MnO_2 nanocomposite may be attributed to surface-mediated interactions, where the large surface area of the starch matrix and its chelating groups help neutralize free radicals. Previous studies [31] have shown that MnO_2 nanoparticles stabilized with bovine serum albumin (BSA-MnO_2 NPs) exhibit enzyme-mimicking antioxidant behaviour, demonstrating activities similar to superoxide dismutase, catalase and peroxidase in various *in vitro* assays. A similar mechanism may operate in rice starch-MnO_2 nanocomposites, where interactions between MnO_2, starch functional groups and free radicals contribute to the overall antioxidant response. Although the inhibitory effect is weaker than the standard, the composite still demonstrates measurable free-radical scavenging potential, likely influenced by the coordinated activity of the metal oxide nanoparticles and the starch matrix.

Conclusion

In this study, starch-MnO_2 nanocomposites were synthesized *via* a green approach using the biodegradable polymer rice starch (PEG 4000) and methanolic extract of soapnut

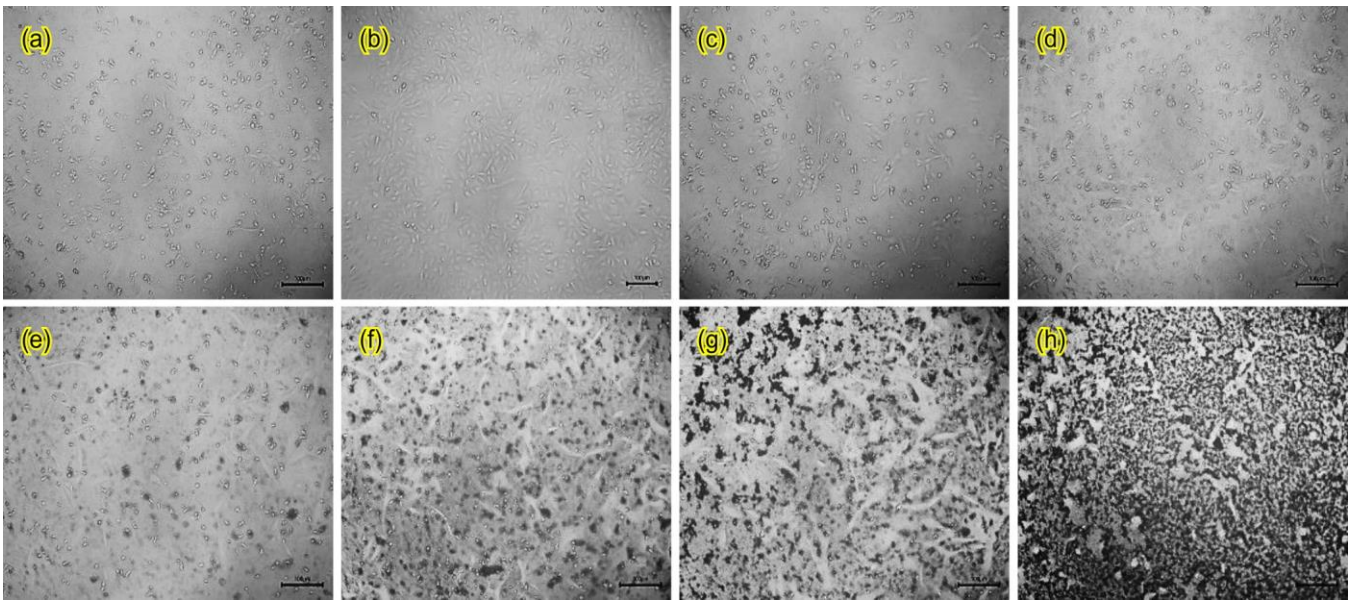

Fig. 8. Morphology of treated HepG2 cell line rice starch-MnO_2 nanocomposite: (a) represents the sample in control, (b to h) shows different concentrations from (b) 1 µg/mL, (c) 10 µg/mL, (d) 50 µg/mL, (e) 100 µg/mL, (f) 250 µg/mL, (g) 500 µg/mL, (h) 1000 µg/mL

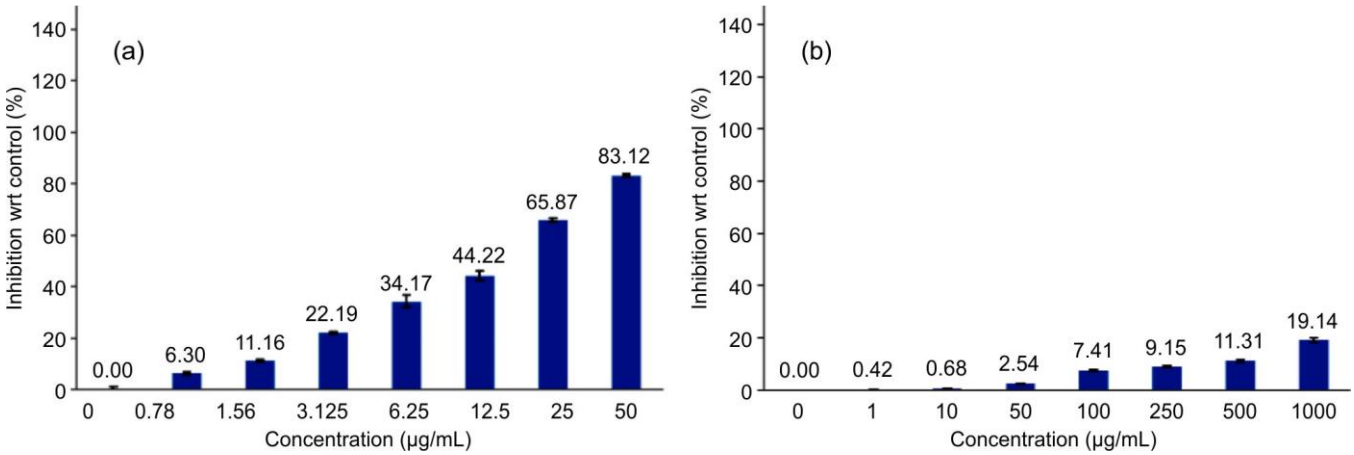

Fig. 9. Graph of antioxidant activity of (a) ascorbic acid, a standard compound, (b) rice starch-MnO_2 nanocomposite plotted between sample concentration *vs.* % inhibition w.r.t. control

(*Sapindus mukorossi*) in an aqueous metal salt solution at room temperature. The resulting nanocomposites exhibited an average crystallite size of 38.27 nm. The biological potential of the synthesized nanocomposites was evaluated in terms of both anticancer and antioxidant activities. MnO_2 nanocomposites stabilized by rice starch and its secondary metabolites, acting as natural reducing and capping agents, demonstrated improved performance under stable thermal conditions. Overall, the findings highlight a promising strategy for generating bioactive rice starch-MnO_2 nanocomposites with significant anticancer and antioxidant properties, suggesting their potential for diverse biomedical applications.

ACKNOWLEDGEMENTS

The authors are grateful to their management and the UGC-CSIR for the financial support and to the MNIT MRC, Jaipur, India, for providing the analytical instrumentation facilities. The authors acknowledge Aakaar Biotechnologies Pvt. Ltd., Lucknow, India, for biological activity analysis and SAIF, Panjab University, Chandigarh, for FESEM-EDX and zeta potential analysis. Special thanks are extended to Retd. Prof. R.N. Mehrotra, former Head, Department of Chemistry, Jodhpur University, for his valuable guidance during the research.

CONFLICT OF INTEREST

The authors declare that there is no conflict of interests regarding the publication of this article.

DECLARATION OF AI-ASSISTED TECHNOLOGIES

During the preparation of this manuscript, the authors used an AI-assisted tool(s) to improve the language. The authors reviewed and edited the content and take full responsibility for the published work.

REFERENCES

1. W.M. Saod, L.L. Hamid, N.J. Alaallah and A. Ramizy, *Biotechnol. Rep.*, **34**, e00729 (2022); https://doi.org/10.1016/j.btre.2022.e00729.
2. H.Y. Xia, B.Y. Li, Y. Zhao, Y.H. Han, S.B. Wang, A.Z. Chen and R.K. Kankala, *Coord. Chem. Rev.*, **464**, 214540 (2022); https://doi.org/10.1016/j.ccr.2022.214540
3. A. Greene, J. Hashemi and Y. Kang, *Nanotechnology*, **32**, 025713 (2021); https://doi.org/10.1088/1361-6528/abb626
4. Y. Chen, H. Cong, Y. Shen and B. Yu, *Nanotechnology*, **31**, 202001 (2020); https://doi.org/10.1088/1361-6528/ab6fe1
5. H. Lu, X. Zhang, S.A. Khan, W. Li and L. Wan, *Front. Microbiol.*, **12**, 761084 (2021); https://doi.org/10.3389/fmicb.2021.761084
6. R.R. Muthuchudarkodi and C. Vedhi, *Appl. Nanosci.*, **5**, 481 (2015); https://doi.org/10.1007/s13204-014-0340-3
7. I. khan, E. Laiq and U. Meraj, *Orient. J. Chem.*, **41**, 758 (2025); https://doi.org/10.13005/ojc/410307
8. L. Umaralikhan and M.J. Mohamed Jaffar, *Iran. J. Sci. Technol. Trans. A Sci.*, **42**, 477 (2018); https://doi.org/10.1007/s40995-016-0041-8
9. A.A. Shaikh, P. Datta, P. Dastidar, A. Majumder, M.D. Das, P. Manna and S. Roy, *J. Polym. Eng.*, **44**, 83 (2024); https://doi.org/10.1515/polyeng-2023-0166
10. A. Ghazzy, R.R. Naik and A.K. Shakya, *Polymers*, **15**, 2167 (2023); https://doi.org/10.3390/polym15092167
11. B. Prill and S. Yusan, *Particul. Sci. Technol.*, **40**, 521 (2022); https://doi.org/10.1080/02726351.2021.1967536
12. H.E. Ali, M.M. Abdel-Aziz, A.M. Aboraia, I.S. Yahia, H. Algarni, V. Butova, A.V. Soldatov and Y. Khairy, *Optik*, **227**, 165969 (2021); https://doi.org/10.1016/j.ijleo.2020.165969
13. R. Ahmed, H. Tahir, M. Saad, M. Latif, A. K. Tanoli and T. Haider, *Iran. J. Chem. Chem. Eng*, **42**, (2023).
14. D. Souza, A.F. Sbardelotto, D.R. Ziegler, L.D.F. Marczak and I.C. Tessaro, *Food Chem.*, **191**, 36 (2016); https://doi.org/10.1016/j.foodchem.2015.03.032
15. S.S. Majani, S. Sathyan, M.V. Manoj, N. Vinod, S. Pradeep, C. Shivamallu, V. K.N and S.P. Kollur, *Curr. Res. Green Sustain. Chem.*, **6**, 100367 (2023); https://doi.org/10.1016/j.crgsc.2023.100367
16. R. Kizil, J. Irudayaraj and K. Seetharaman, *J. Agric. Food Chem.*, **50**, 3912 (2002); https://doi.org/10.1021/jf011652p
17. D. Fan, W. Ma, L. Wang, J. Huang, J. Zhao, H. Zhang and W. Chen, *Stärke*, **64**, 598 (2012); https://doi.org/10.1002/star.201100200
18. M. Ahmad, A. Gani, I. Hassan, Q. Huang and H. Shabbir, *Sci. Rep.*, **10**, 3533 (2020); https://doi.org/10.1038/s41598-020-60380-0
19. I. Govindaraju, G.-Y. Zhuo, I. Chakraborty, S.K. Melanthota, S.S. Mal, B. Sarmah, V.J. Baruah, K.K. Mahato and N. Mazumder, *Food Hydrocoll.*, **122**, 107093 (2022); https://doi.org/10.1016/j.foodhyd.2021.107093
20. P.V. Kowsik and N. Mazumder, *Microsc. Res. Tech.*, **81**, 1533 (2018); https://doi.org/10.1002/jemt.23160
21. A. Kumar, M.S. Aathira, U. Pal and S.L. Jain, *ChemCatChem*, **10**, 1844 (2018); https://doi.org/10.1002/cctc.201701470
22. M.Z. Rong, M.Q. Zhang and W.H. Ruan, *Mater. Sci. Technol.*, **22**, 787 (2006); https://doi.org/10.1179/174328406X101247
23. J. Henry, K. Mohanraj, S. Kannan, S. Barathan and G. Sivakumar, *Walailak J. Sci. Technol.*, **11**, 437 (2014).
24. M.E. Abd El-Aziz, S.M.M. Morsi, M.S. Hasanin and A.M. Youssef, *Carbohydr. Polym. Technol. Appl*, **10**, 100789 (2025); https://doi.org/10.1016/j.carpta.2025.100789
25. P. Yadav, R.T. Olsson and M. Jonsson, *Radiat. Phys. Chem.*, **78**, 939 (2009); https://doi.org/10.1016/j.radphyschem.2009.02.006
26. M. Ganesan, C. Muthaiah, M.A. Wadaan, M. Kumar, D.H.Y. Yanto, S. Kumar, T. Selvankumar, A. Arulraj, R.V. Mangalaraja and S. Suganthi, *Luminescence*, **39**, e4875 (2024); https://doi.org/10.1002/bio.4875
27. I. Ullah, A. Kamal, M. Saba, U. Ara, D. Touhami, A. Wahab, T. Maqbool, M. Nazish, A.F. Alrefaei and M. Lackner, *Sci. Rep.*, **15**, 23696 (2025); https://doi.org/10.1038/s41598-025-93818-4
28. Y. Ji, Y. Wang, X. Wang, C. Lv, Q. Zhou, G. Jiang, B. Yan and L. Chen, *J. Hazard. Mater.*, **468**, 133800 (2024); https://doi.org/10.1016/j.jhazmat.2024.133800
29. K. Manimaran, D.H.Y. Yanto, M. Govindasamy, B. Karunanithi, F.A. Alasmary and R.A. Habab, *Biomass Convers. Biorefin.*, **14**, 12575 (2024); https://doi.org/10.1007/s13399-023-04382-8
30. H.H. Farhan and A.M. Mohammed, *Results Chem.*, **7**, 101266 (2024); https://doi.org/10.1016/j.rechem.2023.101266
31. S. Pardhiya, E. Priyadarshini and P. Rajamani, *SN Appl. Sci.*, **2**, 1597 (2020); https://doi.org/10.1007/s42452-020-03407-5